

# Structures and Photophysical Properties of Model Compounds for Arylethylene Disilylene Polymers

Hong Li, Douglas R. Powell, Timothy K. Firman, and Robert West\*

Department of Chemistry, University of Wisconsin—Madison, 1101 University Avenue, Madison, Wisconsin 53706

Received July 28, 1997; Revised Manuscript Received November 10, 1997

**ABSTRACT:** The compounds  $[C_6H_5C\equiv CC_6H_4C\equiv CSiR_2]_2$  ( $R = Me$  (**3a**),  $n$ -Bu (**3b**)) have been synthesized by the reaction of  $C_6H_5C\equiv CC_6H_4I$  with  $HC\equiv CSiR_2SiR_2C\equiv CH$ . The structures of  $[C_6H_5C\equiv CSi(CH_3)_2]_2$  (**2**), **3a**, and  $C_6H_5C\equiv CC_6H_4C\equiv CC_6H_5$  (**4**) have been determined by a single-crystal X-ray diffraction. In **3a** and **4** short contact distances between the aryl rings and the acetylene groups (3.587 (3) Å in **3a** and 3.481 (2) Å in **4**) indicate strong intermolecular interactions in the solid state. The fluorescence spectra of diphenylacetylene, **3a**, **3b**, and **4** are highly dependent on concentration. In dilute solution (around  $10^{-6}$  mol/L), spectra appear to be of single molecules, but at higher concentration, a red shift was observed, assigned to excimer formation. At still higher solid-state concentrations or in crystals, a further red shift for **3a** and **4** was evident, probably due to the formation of aggregates.

## I. Introduction

Linear conjugated polymers with alternating aryl and acetylenic groups form a new family of rigid rod polymers.<sup>1</sup> Because of their photoluminescent and electroluminescent properties, these polymers have potential for application in light-emitting electroluminescent devices, especially for large-area light-emitting displays.<sup>2</sup>

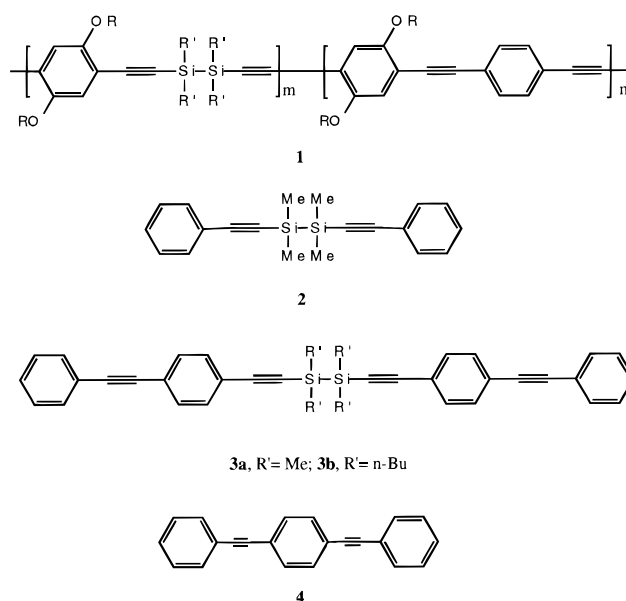
However, the polarizable  $\pi$  electrons of rigid rod conjugated polymers lead to strong intermolecular interaction, and unsubstituted macromolecules of high molecular weight are often insoluble and infusible. Several strategies have been developed to overcome this difficulty. To increase the solubility and simultaneously the molecular weight of polymers, long side chains such as  $n$ -C<sub>12</sub>H<sub>25</sub> and  $n$ -C<sub>16</sub>H<sub>33</sub> alkyl groups have been attached.<sup>3</sup> To increase chain flexibility, groups such as  $(CH_2)_n$  have been included into the main chain of otherwise rigid rod polymers.<sup>4</sup> The approach in our laboratories has been the introduction of  $(SiR_2)_n$  groups into the aryl–acetylene polymer chains.<sup>5</sup> This combination provides alternating delocalized  $\sigma$ -bonds and  $\pi$ -bonds in the main chain, which may partially preserve the extended delocalization while increasing the flexibility of the polymers. These rod–coil polymers **1** can be formed into films more easily than rigid rod polymers, which may be important in their practical application.

In this paper, we report the synthesis and characterization of **2**, **3a**, **3b**, and **4** and the crystal structures of **2**, **3a**, and **4**, as model compounds for polymers **1**. Since polymers **1** are strongly fluorescent, the photoproperties of **2**, **3a**, **3b**, and **4** were also investigated in some detail.

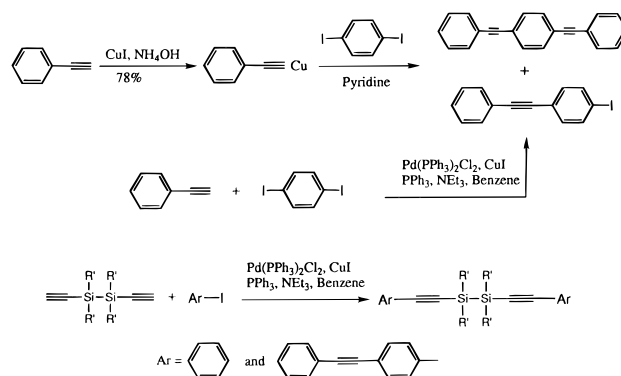
## II. Results and Discussion

Diphenylethynylenetetramethyldisilane (**2**),<sup>6</sup> 1,1,2,2-tetramethyl-1,2-diethynyldisilane, and 1,1,2,2-tetra- $n$ -butyl-1,2-diethynyldisilane<sup>7</sup> were synthesized following procedures described in the literature.

4-Phenylethynyleneiodobenzene (**5**) was synthesized by the palladium-catalyzed cross-coupling<sup>8</sup> of diiodobenzene with phenylacetylene or alternatively by the reaction of copper(I) phenylacetylide with  $p$ -diiodobenzene.<sup>4</sup> **4**<sup>9</sup> was also produced in the same reactions. Reaction of the 1,2-diethynyltetraalkyldisilane with **5** gave compounds **3a** and **3b**, as shown in Scheme 1.



Scheme 1



**X-Ray Crystal Structures.** A single crystal of **4** was obtained by sublimation, and the crystal structure was determined. Two views of the molecule are shown in Figure 1. The aromatic rings are coplanar, and the molecule is very nearly linear with dihedral angles between the triple bonds and adjacent carbon atoms of 179.3 (2)°, 178.1(2)°, 179.4 (2)°, and 179.6 (2)°. The structure thus resembles that of diphenylacetylene,<sup>10</sup>

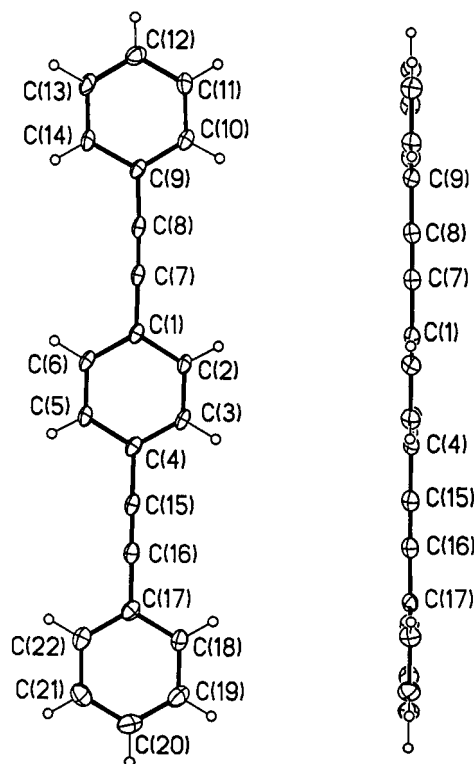


**Figure 1.** Crystal structure of **4** with selected bond distances (Å) and angles (deg):<sup>17</sup> C(7)–C(8), 1.201(2); C(8)–C(9), 1.433(2); C(9)–C(10), 1.395(2); C(8)–C(7)–C(1), 179.3(2); C(7)–C(8)–C(9), 178.1(2).

which is also planar and nearly linear in the solid state. The crystal packing diagram for **4** is shown in Figure 2. The molecules stack in such a way that each C≡C bond is close to a C=C bond of an aromatic ring on a neighboring molecule. The shortest intermolecular carbon–carbon contact distance, 3.481 (2) Å, is between C(2) and C(9)' ( $1 - x, 2 - y, 1 - z$ ), suggesting strong intermolecular interaction between the aromatic ring systems in the solid state. Crystal data for compounds **2**, **3a**, and **4** are shown in Table 1.

The X-ray structure of **2** is shown in the thermal ellipsoid diagram of Figure 3. The crystals contain two nonequivalent molecules, each with a crystallographically imposed center of symmetry. Bond distances and angles are identical within the experimental limits for both molecules. The angles C(2A)–C(1A)–Si(1A) (178.7 (2)°) and C(1A)–C(2A)–C(3A) (177.0 (2)°) are close to 180°, so the arrangement at the triple bonds is almost linear. The two phenylethynyl groups are trans to one another; molecular models indicate that this is the most stable conformation. The shortest intermolecular contact distance in **2** is 3.631 (3) Å, between C(9A) and C(3A)' ( $1 - x, 1 - y, 1 - z$ ), a methyl carbon and a phenyl carbon. There are no close  $\pi$ – $\pi$  intermolecular interactions.

Compounds **3a** and **3b** provide the best models for aryethynylene disilylene polymers. Single crystals of **3a** were obtained by recrystallization from ethanol; the structure of **3a** is shown in Figure 4, and a packing diagram is displayed in Figure 5. The bond angles C(2)–C(1)–Si(1) (169.9 (2)°) and of C(9)–C(10)–C(11) (174.9 (2)°) are significantly smaller than 180°, and the aryl groups connected by the acetylene groups are far from coplanar, with a dihedral angle between them of 62.9 (2)°. Thus the conformation is very different from

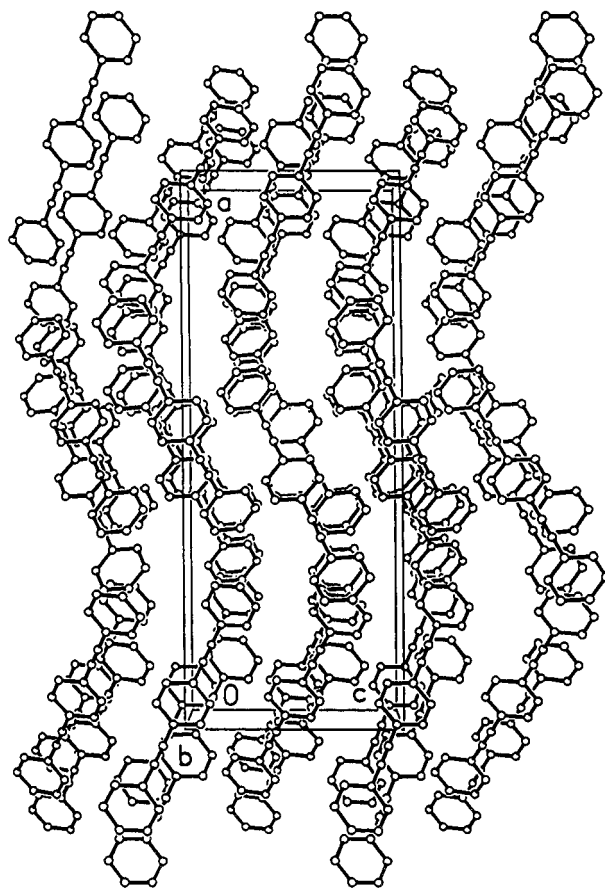


**Figure 2.** Packing diagram of **4**.

that in **4**. It is interesting to note that the intermolecular aryl groups are not directly stacked over each other but are closer to the acetylene groups of the adjacent molecules. The shortest intermolecular carbon–carbon contact distance is 3.587 (3) Å between C(9) of one molecule and C(14)' ( $2 - x, y - 1/2, 1/2 - z$ ) in another molecule, consistent with significant intermolecular interaction in the solid state.

**UV and Fluorescence Spectra.** The UV spectra of **3a** and **3b** in THF solution are shown in Figure 6. Two peaks were observed at 306 nm ( $\epsilon = 1.18 \times 10^4$ ) and 326 nm ( $\epsilon = 1.13 \times 10^4$ ) for **3a** and at 308 nm ( $\epsilon = 1.07 \times 10^4$ ) and 328 nm ( $\epsilon = 1.03 \times 10^4$ ) for **3b**. Compared with those of compound **2** (248 and 259 nm),<sup>6</sup> the peaks of **3a** are red shifted about 58 and 67, nm respectively. Both **3a** and **3b** have a peak at 332 nm and a broad shoulder around 350 nm in the emission spectra in dilute solution. The similarity of the spectra of **3a** and **3b** indicates that changing the side chain on the Si backbone has little apparent effect on the photoproperties of these molecules.

The fluorescence spectrum of **4** has been published, but there is no report on the concentration dependence of the spectrum.<sup>11</sup> Our results (Figures 7 and 8) show that the photoproperties of **4** depend strongly on concentration. In dilute solution in THF, the band with the greatest intensity was a sharp peak at 347 nm. Other peaks, at 364 and 375 nm, were observed with lower intensities. As the concentration increased, the peak at 347 nm gradually disappeared, and the peaks at 364 and 375 nm became larger. Different solvents such as  $\text{CHCl}_3$  were also used, and the results were quite similar to those in THF. The emission spectra of a thin film of polystyrene containing 3% of **4** showed a

Table 1. Summary of Crystal Data and Structure Refinement for 2, 3a, and 4

	2	3a	4
empirical formula	C <sub>20</sub> H <sub>22</sub> Si <sub>2</sub>	C <sub>36</sub> H <sub>30</sub> Si <sub>2</sub>	C <sub>22</sub> H <sub>14</sub>
crystal color	colorless	colorless	colorless
crystal size (mm)	0.38 × 0.22 × 0.20	0.52 × 0.14 × 0.12	0.48 × 0.44 × 0.08
crystal system	triclinic	monoclinic	orthorhombic
space group	<i>P</i> $\bar{1}$	<i>P</i> 2 <sub>1</sub> / <i>c</i>	<i>Pbcn</i>
<i>a</i> (Å)	8.1477(5)	7.4518(2)	28.1212(9)
<i>b</i> (Å)	11.0606(6)	5.9376(2)	9.3300(3)
<i>c</i> (Å)	12.5047(8)	33.7569(10)	11.0541(3)
$\alpha$ (deg)	102.425	90	90
$\beta$ (deg)	107.453	91.6798	90
$\gamma$ (deg)	109.297	90	90
volume (Å <sup>3</sup> )	950.81(10)	1492.96(8)	2900.3(2)
peaks to determine cell	4126	4593	4904
$\theta$ range of cell peaks (deg)	3.0–25.5	3.0–25.0	3.0–25.0
temp (K)	133(2)	133(2)	133(2)
wavelength (Å)	0.710 73	0.710 73	0.710 73
<i>Z</i>	2	2	8
formula weight	318.56	518.78	278.33
density (g cm <sup>-3</sup> )	1.113	1.154	1.275
absorption coefficient (mm <sup>-1</sup> )	0.182	0.141	0.072
<i>F</i> (000)	340	548	1168
$\theta$ range for collection (deg)	1.82–25.82	2.41–28.24	1.45–28.43
<i>h</i>	–9 ≤ <i>h</i> ≤ 9	–9 ≤ <i>h</i> ≤ 9	–35 ≤ <i>h</i> ≤ 21
<i>k</i>	–13 ≤ <i>k</i> ≤ 12	–7 ≤ <i>k</i> ≤ 2	–12 ≤ <i>k</i> ≤ 11
<i>l</i>	–15 ≤ <i>l</i> ≤ 14	–41 ≤ <i>l</i> ≤ 43	–6 ≤ <i>l</i> ≤ 14
standard peaks	86	144	110
no. of reflns collected	5407	6244	12368
no. of indep reflns ( <i>R</i> <sub>int</sub> )	3095 (0.028)	3173 (0.0325)	3351(0.0612)
good-of-fit on <i>F</i> <sup>2</sup>	1.100	1.145	1.004
<i>R</i> ( <i>F</i> ), <i>wR</i> <sub>2</sub> [ <i>I</i> > 2σ( <i>I</i> )]	0.0430, 0.1204	0.0607, 0.1191	0.0541, 0.1241
<i>R</i> ( <i>F</i> ), <i>wR</i> <sub>2</sub> (all data)	0.0561, 0.1258	0.0782, 0.1261	0.1018, 0.1489
(Δρ) <sub>max,min</sub> (eÅ <sup>-3</sup> )	0.352, –0.326	0.341, –0.319	0.254, –0.279

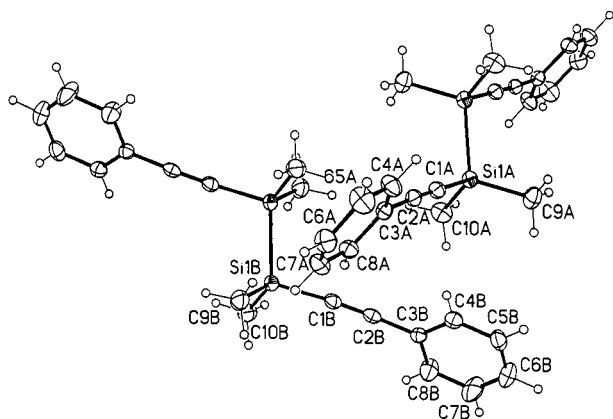


**Figure 3.** Crystal structure of diphenylethynyltetramethyldisilane (**2**) with selected bond distances (Å) and angles (deg): Si(1A)–C(1A), 1.841(2); Si(1A)–C(10A), 1.857(2); Si(1A)–Si(1A), 2.3289(12); C(1A)–C(2A), 1.204(3); C(2A)–C(3A), 1.437(3); C(2A)–C(1A)–Si(1A), 178.7(2); C(1A)–C(2A)–C(3A) 177.0(2).

peak with highest intensity at 371 nm, as well as a peak at 355 nm; the major peak shifted to 383 nm in the emission spectrum of a film containing 20% of **4**. The emission spectrum of a film of pure **4** has four peaks at 386, 393, 412, and 420 nm, quite strongly red shifted, compared to those of the dilute solution.

The emission band at 347 nm in dilute solution can reasonably be assigned to single molecules. Increasing the concentration apparently leads to increased intermolecular interaction, until an excimer<sup>12</sup> is formed (a sandwiched excited dimer<sup>13</sup> formed by the interaction of the ground state of **4** with the excited molecule). As a result, the peaks in the fluorescence spectra are red shifted. When the concentration is further increased, aggregates (as shown in the packing diagram of Figure 5) may interact with the excited molecules. Thus a more

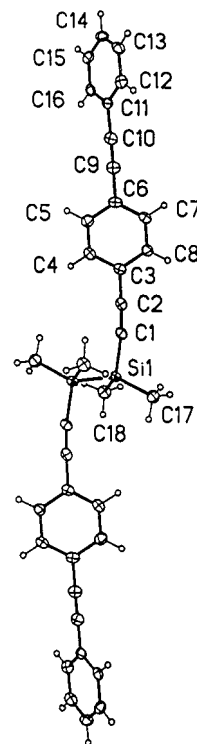


**Figure 4.** Crystal structure of **3a** with selected bond distances (Å) and angles (deg): Si(1)–C(1), 1.854(2); Si(1)–C(17), 1.876(2); Si(1)–Si(1), 2.3498(12); C(1)–C(2), 1.206(3); C(2)–C(3), 1.450(3); C(2)–C(1)–Si(1), 169.9(2); C(1)–C(2)–C(3), 176.9(2); C(10)–C(9)–C(6), 178.7(3); C(9)–C(10)–C(11), 174.9(2).

complicated excited-state structure containing an excimer core<sup>14</sup> may form, causing the fluorescence spectra to be even more red shifted.

The emission spectra of **3a** at different concentrations are shown in Figure 9. In dilute solution, an emission

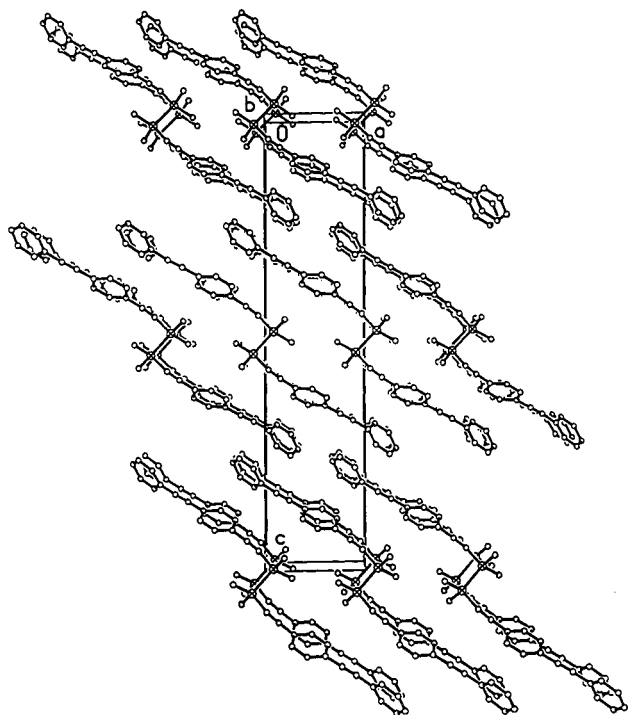


**Figure 5.** Packing diagram of **3a**.

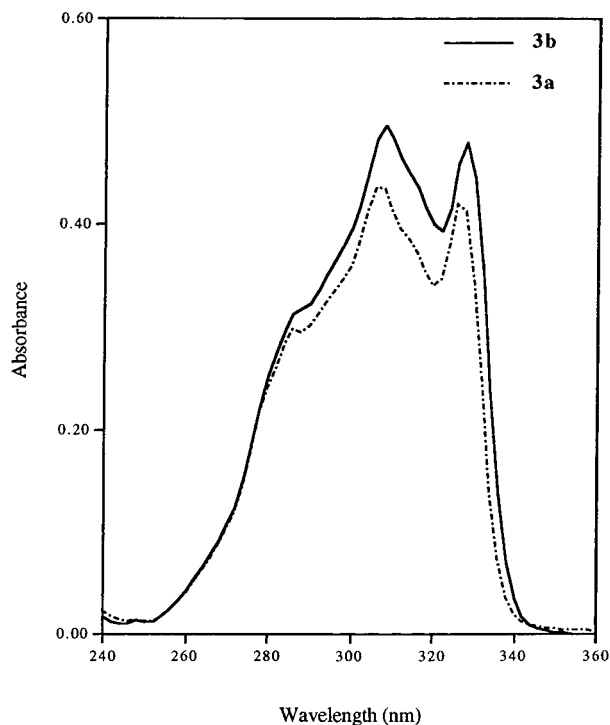


**Figure 6.** UV absorption spectra of **3a** ( $3.70 \times 10^{-6}$  mol/L) and **3b** ( $4.65 \times 10^{-6}$  mol/L) in THF.

band with peaks at 332 and 348 nm was observed. As the concentration increased to 0.5 wt % in polystyrene film, an emission band with peaks at 345 nm was observed. However, the peak at 332 nm completely disappeared. The emission bands of crystals of **3a** are quite red shifted with peaks at 382 and 398 nm. It is evident from Figure 9 that as the concentration increased, the relative intensity of the peak at 347 nm decreased, while the relative intensity of the peak at 398 nm increased.

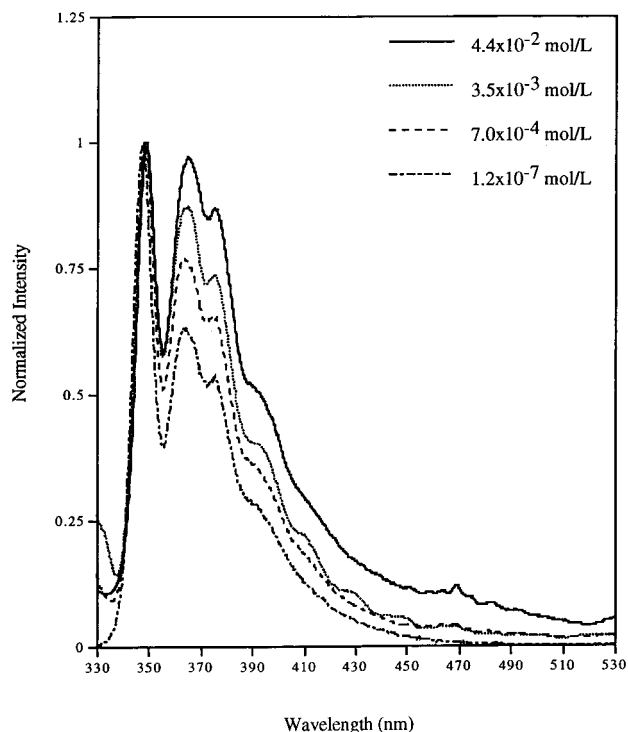


**Figure 7.** Emission spectra of **4** at different concentrations in THF.

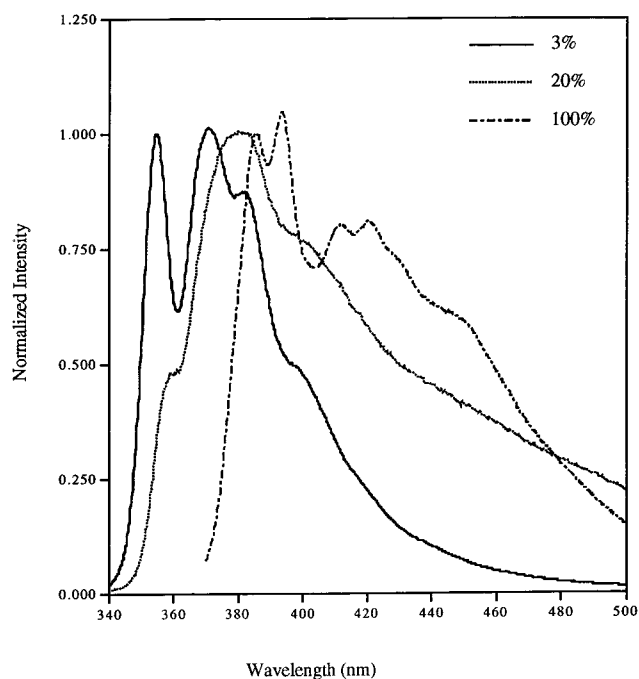


**Figure 8.** Thin film emission spectra of **4** at different concentrations in polystyrene films.

The emission band with a peak at 332 nm can be assigned to single molecules. We propose that as the concentration is increased, excimers of **3a** (with partially sandwiched structure due to the nonplanar structure of **3a**) are formed which are good light emitters, so the fluorescence intensities of the moderately concentrated solution are similar to those of the dilute solution. Upon further increasing the concentration or in crystals, the fluorescence bands were shifted to longer wavelengths, which suggests the formation of aggregates in the ground state and more complicated structures (containing an excimer core) in the excited state. The concen-

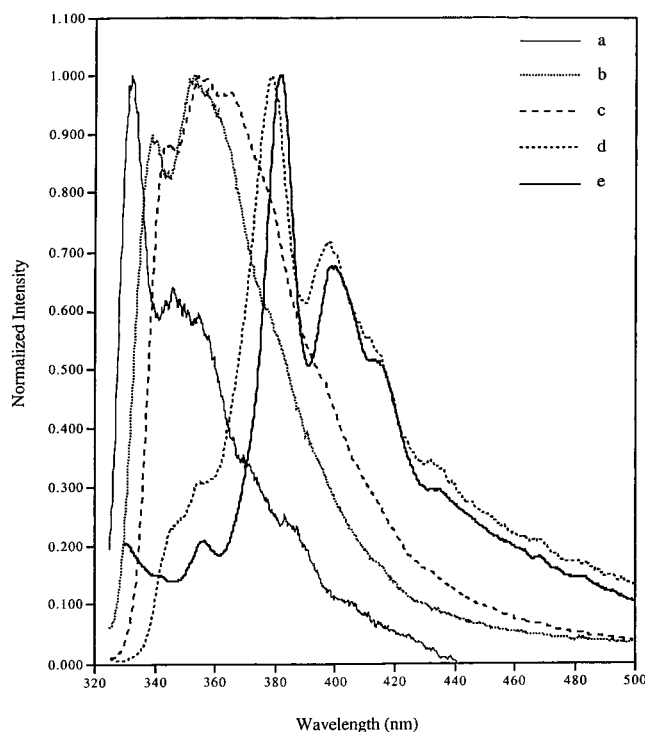


**Figure 9.** Emission spectra of **3a** in THF and in polystyrene films at different concentrations: (a)  $3.70 \times 10^{-6}$  mol/L in THF solution; (b) 0.5% in polystyrene; (c) 2.3% in polystyrene; (d) 26.8% in polystyrene; (e) 100% crystal.

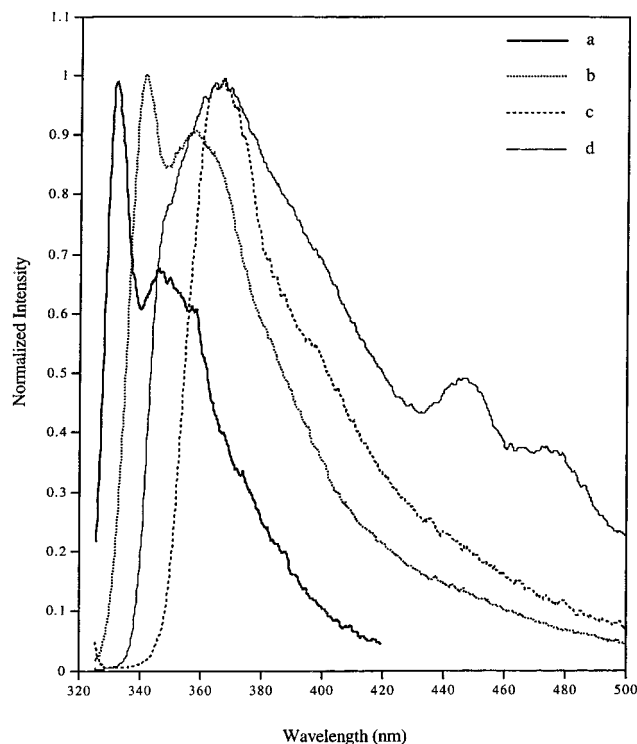


**Figure 10.** Emission spectra of **3b** in THF and in polystyrene films at different concentrations: (a)  $1.80 \times 10^{-6}$  mol/L in THF solution; (b) 3% in polystyrene; (c) 31.7% in polystyrene; (d) 100% crystal.

tration-dependent emission spectra of **3b** are shown in Figure 10. The spectra in dilute solution were similar to those of **3a**. However, in concentrated solid-state solution or crystals, the emission peak was only slightly red shifted to 367 nm. The formation of an excimer core

may be limited due to the longer *n*-butyl substituent group.

Both compounds, when irradiated continuously at 325 nm in film, appear to undergo a photoreaction. The major peak gradually decreased, and a new emission band around 450 nm was observed. After photolysis at 254 nm for 18 h in THF, the proton NMR spectra of **3a** and **3b** became very complicated, indicating that a complex mixture is formed.

### III. Conclusions

The planar structure of **4** and the short intermolecular contact distance (3.481 (2) Å) between aryl rings and acetylenes indicate aggregate formation in the solid state. The single-crystal structure of compound **3a** clearly shows that the 4-phenylethynylphenylene group does not have a planar structure but is bent with a dihedral angle of 62.9 (2)° and that the Si–C≡C angle is not 180° but 169.9 (2)°. The short intermolecular contact distance (3.587 (3) Å) between C(9) and C(14) indicates a strong intermolecular interaction, which leads to excimer and aggregate formation in solution and in the solid state.

Whether the structure is planar or not, the fluorescence spectra of **3a**, **3b**, and **4** are highly dependent on concentration. The molecular fluorescence spectra were observed in dilute solution, while longer wavelength emission bands were observed when the solute concentration was increased. At still higher concentrations or in crystals, further red shifts of the fluorescence spectra of **3a** and **4** suggest aggregate formation.

### IV. Experimental Section

**General Procedure.** Proton, carbon, and silicon nuclear magnetic resonance ( $^1\text{H}$ ,  $^{13}\text{C}$ , and  $^{29}\text{Si}$  NMR) spectra were recorded in deuterated solvent on a Bruker WP-300 (300 MHz for  $^1\text{H}$  NMR, 75 MHz for  $^{13}\text{C}$  NMR) and a Bruker AM-500 (500 MHz for  $^1\text{H}$  NMR, 125.3 MHz for  $^{13}\text{C}$  NMR, and 99.36 MHz for  $^{29}\text{Si}$  NMR). Absorption spectra were measured with a Hewlett-Packard 8452A diode array spectrophotometer. Fluorescence emission and excitation spectra were recorded on a Hitachi Model F-4500 fluorescence spectrophotometer. For measuring the concentration-dependent fluorescence spectra, a series of cells with different path lengths from 1.0 to 0.015 cm were used. The films with different concentrations in polystyrene were made by dissolving polystyrene (average MW 45 000, Aldrich Chemical Co., Inc.) and compound **3a**, **3b**, or **4** in THF and then coating that solution on a glass plate. All reactions were performed under  $\text{N}_2$  or Ar atmosphere.

**X-ray Structure Determinations.** The X-ray crystallographic analysis was based on data collected on a Siemens P4 diffractometer equipped with a graphite crystal monochromator and a CCD area detector. Mo K $\alpha$  radiation ( $\lambda = 0.71073$  Å) was used for **2**, **3a**, and **4**. Suitable crystals of **4** were obtained from sublimation at 200 °C/0.1 Torr; crystals of **2** and **3a** were grown from ethanol at 25 °C. The orientation matrices and unit cell parameters were determined by the least-squares fitting of 4904 reflections and  $3.0^\circ < \theta < 25.0^\circ$  for **4**, 4126 reflections and  $3.0^\circ < \theta < 25.5^\circ$  for **2**, and 4593 reflections and  $3.0^\circ < \theta < 25.0^\circ$  for **3a**. The intensity of the standard reflections had a maximum variation of 0.08%–0.41%. All the structures were solved using the SHELXS-86 program.<sup>15</sup> The non-hydrogen atoms were refined anisotropically using the SHELXS-93 program<sup>16</sup> by full-matrix least-squares analysis on  $F^2$ . The applied weighting scheme for all the structures was  $w^{-1} = \sigma^2 F_o^2 + (xP)^2 + yP [P = (F_o^2 + 2F_c^2)/3]$ ,<sup>16</sup> where  $x = 0.0634$  and  $y = 0.0$  for **4**,  $x = 0.0651$  and  $y = 0.0333$  for **2**, and  $x = 0.0275$  and  $y = 1.1566$  for **3a**.

**Synthesis of 4-Phenylethynylbenziodobenzene and 4.** In a 250-mL three-necked flask with a magnetic stir bar, 1,4-diiodobenzene (6.6 g, 0.020 mol), benzene (150 mL), Pd(PPh<sub>3</sub>)<sub>2</sub>

Cl<sub>2</sub> (0.015 g), PPh<sub>3</sub> (0.15 g), CuI (0.015 g), and NEt<sub>3</sub> (20 mL) were combined. Phenylacetylene (2.0 g, 0.020 mol) in 20 mL of benzene was added in 1 h. The reaction was carried out for 24 h, and the mixture was filtered to remove salts. The solvent was removed under vacuum, and the residue was column chromatographed on silica gel, eluting with THF to remove the catalysts. The solvent was removed under vacuum, the residue was sublimed to remove unreacted diiodobenzene (24% recovered), and the resulting residue was recrystallized from hexane. The product sublimed at 200 °C at 0.1 Torr, giving 1.8 g (32%) of **4** as clear colorless crystals. The remaining hexane solution was concentrated and then purified by column chromatography with hexane as the eluent, and the first component was recrystallized from ethanol, giving 2.5 g (38%) of 4-phenylethynylidobenzene. <sup>1</sup>H NMR (CDCl<sub>3</sub>, ppm) δ: 7.28 (2H, dt), 7.45 (5H, m), 7.72 (2H, dt). <sup>13</sup>C NMR δ: 91.04, 94.41, 123.19, 128.84, 128.98, 131.92, 133.43, 138.01.

**Synthesis of 3a.** In a 100-mL Schlenk flask equipped with a condenser, 4-phenylethynylidobenzene (1.0 g, 3.3 mmol), 1,1,2,2-tetramethyl-1,2-diethynyldisilane (0.22 g, 1.6 mmol), a catalytic amount of Pd(PPh<sub>3</sub>)<sub>2</sub>Cl<sub>2</sub>, CuI, and PPh<sub>3</sub>, 10 mL of NEt<sub>3</sub>, and 50 mL of benzene were combined. The mixture was stirred for 24 h at room temperature, and the salts were removed by filtration. The solvent was removed under vacuum, and the residue was recrystallized in 100 mL of hexane, giving 0.60 g (72%) of compound **3a**, mp 163–164 °C. <sup>1</sup>H NMR (300 MHz, C<sub>6</sub>D<sub>6</sub>, ppm) δ: 0.48 (s, 12H), 6.95 (m, 6H), 7.29 (m, 8H), 7.49 (m, 4H). <sup>13</sup>C NMR (75 MHz, C<sub>6</sub>D<sub>6</sub>, ppm) δ: -2.76, 89.71, 92.07, 94.47, 108.28, 123.45, 123.59, 123.95, 128.63, 131.82, 131.90, 132.26. <sup>29</sup>Si NMR (100 MHz, C<sub>6</sub>D<sub>6</sub>, ppm) δ: -36.36. MS *m/e* (relative intensity) 518 (M<sup>+</sup>, 100), 503 (-Me, 52), 445 (18), 259 (58).

**Synthesis of 3b.** In a 100-mL three-necked flask with a magnetic stir bar, 4-phenylethynylidobenzene (0.60 g, 1.97 mmol), 1,1,2,2-tetra-*n*-butyl-1,2-diethynyldisilane (0.33 g, 0.985 mmol), a catalytic amount of CuI, PPh<sub>3</sub>, Pd(PPh<sub>3</sub>)<sub>2</sub>Cl<sub>2</sub>, 20 mL of NEt<sub>3</sub>, and 50 mL of benzene were combined. The mixture was stirred for 24 h at room temperature. The salts were removed by filtration, and the solvent was removed under vacuum. The residue was column chromatographed with THF; then HPLC was performed with toluene as the eluent. The purified solid was recrystallized from ethanol, giving 0.51 g (75%) of colorless crystals of **3b**, mp 64–65 °C. <sup>1</sup>H NMR (CDCl<sub>3</sub>, ppm) δ: 0.87 (20H, m), 1.5 (16H, m), 7.5 (18H, m). <sup>13</sup>C NMR δ: 12.93, 13.78, 26.50, 27.02, 89.12, 92.07, 93.86, 108.12, 118.17, 123.06, 123.18, 123.37, 128.38, 131.37, 131.62, 131.78. <sup>29</sup>Si NMR (100 MHz, ppm) δ: -32.1. MS *m/e* (relative intensity) 686 (M<sup>+</sup>, 100), 630 (14), 573 (21), 517 (33), 461 (18), 287 (15), 231 (54), 165 (25).

**Acknowledgment.** The authors acknowledge the financial support of the U.S. Office of Naval Research and the NSF (Grant CHE-9310428) and the University of Wisconsin for the purchase of the X-ray instrument and computers. We thank Prof. Josef Michl for helpful discussions.

**Supporting Information Available:** For **2**, **3a**, and **4**, tables giving the structure determination summary, positional and thermal parameters, atomic coordinates, bond distances and angles, anisotropic displacement factors, hydrogen coordinates and isotropic displacement parameters, and torsion angles. For **4**, figure giving the emission spectra at different concentrations in CHCl<sub>3</sub> (24 pages). Ordering information is given on any current masthead page.

## References and Notes

- (1) (a) Rutherford, D. R.; Stille, J. K.; Elliott, C. M.; Reichert, V. R. *Macromolecules* **1992**, *25*, 2294. (b) Sasabe, H.; Wada, T.; Hosoda, H.; Ohkawa, H.; Yamada, A.; Garito, A. F. *Mol. Cryst. Liq. Cryst.* **1990**, *189*, 155.
- (2) Kido, J.; Hayase, H.; Hongawa, K.; Nagai, K.; Okuyama, K. *Appl. Phys. Lett.* **1994**, *65*, 2124.
- (3) (a) Swager, T. M.; Gil, C. T.; Wrighton, M. S. *J. Phys. Chem.* **1995**, *99*, 4886. (b) Moroni, M.; Le Moigne, J.; Luzzati, S. *Macromolecules* **1994**, *27*, 562.
- (4) Osaheni, J. A.; Jenekhe, S. A. *J. Am. Chem. Soc.* **1995**, *117*, 7389.
- (5) Yuan, C.-H.; West, R. *Appl. Organomet. Chem.* **1994**, *8*, 423.
- (6) Horn, K. A.; Grossman, R. B.; Thorne, J. R. G.; Whitenack, A. A. *J. Am. Chem. Soc.* **1989**, *111*, 4809.
- (7) Iwahara, T.; Hayase, S.; West, R. *Macromolecules* **1990**, *23*, 1298.
- (8) Heck, R. F. *Palladium Reagents in Organic Synthesis*; Academic Press: New York, 1990.
- (9) Sladkov, A. M.; Ukhin, L. Y.; Korshak, V. V. *Izv. Akad. Nauk SSSR, Ser. Khim.* **1963**, *12*, 2213.
- (10) Mavridis, A.; Moustakali-Mavridis, I. *Acta Crystallogr.* **1977**, *B33*, 3612.
- (11) (a) Gruzinskii, V. V.; Degtyarenko, K. M.; Kopylova, T. N.; Kuznetsov, A. L.; Novikov, A. N.; Sarycheva, T. A. *Zh. Prikl. Spektrosk.* **1987**, *46*, 52. (b) Nakatsuji, S.; Matsuda, K.; Uesugi, Y.; Nakashima, K.; Akiyama, S.; Fabian, W. *J. Chem. Soc., Perkin Trans. 1* **1992**, 755.
- (12) (a) Birks, J. B.; Christophorou, L. G. *Spectrochim. Acta* **1963**, *19*, 401. (b) Jenekhe, S. A.; Osaheni, J. A. *Science* **1994**, *265*, 765.
- (13) (a) Sadygov, R. G.; Lim, E. C. *Chem. Phys. Lett.* **1994**, *225*, 441. (b) Chandross, E. A.; Dempster, C. J. *J. Am. Chem. Soc.* **1970**, *92*, 704. (c) Chandross, E. A.; Dempster, C. J. *J. Am. Chem. Soc.* **1970**, *92*, 3586. (d) Chandra, A. K.; Lim, E. C. *J. Chem. Phys.* **1968**, *49*, 5066.
- (14) Saigusa, H.; Lim, C. E. *Acc. Chem. Res.* **1996**, *29*, 171.
- (15) Sheldrick, G. M. *Acta Crystallogr.* **1990**, *A46*, 467.
- (16) Sheldrick, G. M. *Macromol. Refinement, Proc. CCP4 Study Weekend* **1996**, 47.
- (17) Figure 1 shows no unusual motion of the atoms perpendicular to the molecular plane; however, atoms C(7), C(8), C(15), and C(16) show a tendency to move in a direction along the bond. This is somewhat unusual and probably suggests that the empirical absorption correction applied to this plate-shaped crystal is not ideal. A reexamination of these displacement parameters and the refinement process revealed no other systematic problems.

MA971126S